INT. J. REMOTE SENSING, 2001, VOL. 22, NO. 6, 987–1004

Typology of atoll rims in Tuamotu Archipelago (French Polynesia) at landscape scale using SPOT HRV images

S. ANDRÉFOUËT[1,2], M. CLAEREBOUDT[3,4], P. MATSAKIS[5], J. PAGÈS[6] and P. DUFOUR[3]

[1] Laboratoire de Géosciences Marines et Télédétection, Université Française du Pacifique, BP 6570 Faaa-Aéroport, Tahiti, French Polynesia
[2] Remote Sensing Biological Oceanography Lab., University of South Florida, Department of Marine Science, 140, 7th Avenue South, St Petersburg, FL 33701, USA
[3] IRD, Centre d'Océanologie de Marseille, rue de la Batterie des Lions, F-1037 Marseille, France
[4] College of Agriculture, Fisheries Dept., Sultan Qaboos University, P.O Box 34, Al-Khad 123, Sultanate of Oman
[5] Institut de Recherche en Informatique de Toulouse, Université Paul Sabatier Toulouse—118, Route de Narbonne 31062 Toulouse Cedex, France
[6] Centre IRD de Tahiti, BP 529 Papeete, Tahiti, French Polynesia

(*Received 31 August 1998; in final form 22 November 1999*)

Abstract. The lagoon of an atoll is separated from the ocean by a rim. As the rim controls the flux of water between ocean and lagoon, its structure is one of the major forcing factors of the biological processes that depend on the renewal rate of lagoonal water. Characterizing rim structure and its degree of hydrodynamic aperture is mandatory for comparing the functioning of different atoll lagoons. This paper characterizes at landscape scale the different types of rims of the atolls of the Tuamotu Archipelago (French Polynesia) using SPOT HRV multi-spectral images. The classification of 117 segments of rims highlights nine different rims. They differ in the relative importance of vegetated, submerged, intertidal and emerged domains. These classes are recognized with accuracy greater than 85% using a simple statistical supervised algorithm. A gradient of hydrodynamic aperture is described, from 0.02%—very closed rim exposed to the north, to 0.65%—wide open rim exposed to dominant southern swell. We show that most of these nine rims have a preferential exposure. According to the direction of the dominant swell in the Tuamotu region, such exposure may explain the structure of the rims and their degree of hydrodynamic aperture. We discuss the implications of these results for research and management.

1. Introduction

Atolls are one of the main types of coral reef structures, in addition to barrier, fringing and bank reefs (Guilcher 1988). Atolls are classically described as the final step of a fringing-barrier-atoll succession, a step where only carbonate material produced by coral and associated organisms is visible. Deep drilling and radio-isotope dating in the structure of the atolls have confirmed two processes through geological times that explain concurrently or independently the general saucer-like morphology of atolls (Guilcher 1988). First, this morphology may derive from subaerial erosion of the

International Journal of Remote Sensing
ISSN 0143-1161 print/ISSN 1366-5901 online
http://www.tandf.co.uk/journals

calcareous platform during a period of emergence following a tectonic uplift or a sea-level fall (Menard 1982, Winterer 1998). The surface dissolution resulted in a central depression and a peripheral rim that were recolonized by coral reef organisms as soon as submergence reoccurred. Second, the saucer-shape was explained by continuous differential growth and erosion rate between peripheral and central living communities, and by different patterns of accretion (Woodroffe *et al.* 1999). Whatever the processes, the resulting rim-lagoon structure has major implications for the biological functioning of an atoll. The atoll may be described as a juxtaposition of three ecological systems: the oceanic outer slope, the lagoon (including water column and bottom) and the rim. The rim and its degree of hydrodynamic aperture control the flux of water between ocean and lagoon at short time-scale (hours and days). Therefore, if we consider physical or biological processes with similar time-scale magnitude (Hatcher *et al.* 1987), reefs with different morphology likely have lagoons with different physical and biological properties. This was documented by Furnas *et al.* (1990), Delesalle and Sournia (1992) and Dufour *et al.* (1998). Landscape ecology aims to describe the influence of structural properties, such as connectivity, degree of overlapping or porosity, on the functioning of ecosystems (Forman and Godron 1986). If we define the landscape scale as the scale that provides the adequate information on connectivity between the ocean and the lagoon, then the landscape scale is required to compare and explain the functioning of different lagoons, in order to link oceanic processes, rim structure and lagoonal biological features.

This study focuses on the characterization of the rim structure of the atolls of Tuamotu Archipelago (14° S–24° S, 134° W–148° W), French Polynesia. Tuamotu includes 77 of the 425 atolls of the world (according to the interpretation by Stoddart (1965) of the list given by Bryan (1953)). The genesis, transformation and present structure of atolls and rims of this archipelago have been studied at several occasions (Stoddart 1969, McNutt and Menard 1978, Montaggioni and Pirazzoli 1984, Bourrouilh-LeJan *et al.* 1985, Bourrouilh-LeJan and Tallandier 1985, Montaggioni *et al.* 1985, Pirazzoli *et al.* 1987, 1988a, 1988b, Perrin 1990, Buigues *et al.* 1992, Ito *et al.* 1995, Stoddart and Murphy 1996). The descriptions generally emphasized geologic processes. They highlighted the influence of oceanic, eustatic, tectonic and catastrophic (hurricanes or tsunamis) processes at different spatial and temporal scale, but these descriptions are not relevant for what we have defined as the landscape scale. For the remote and hard-to-access atolls, remotely sensed SPOT HRV, Landsat TM/ETM+ or IRS1-C LISS-III images seem more suitable to get consistent synoptic information at landscape scale (Quattrochi and Pelletier 1990). Atolls world-wide have received little attention from the remote sensing community (Loubersac *et al.* 1988, 1991, Mumby et al 1995). In Tuamotu, bathymetric modelling (Pirazzoli 1984, Fourgassié 1990) and geomorphology mapping (Salvat *et al.* 1990, Loubersac 1994) have been carried out but not systematically despite a databank of SPOT-HRV multi-spectral images covering 51 of the 77 atolls (figure 1).

We describe in this study how these SPOT HRV images were processed to characterize rims of the Tuamotu atolls at landscape scale in structure, degree of aperture and exposure. We discuss the potential interest of the classification of rims for research and management.

2. Material and methods

2.1. *Defining a typology of rims*

In order to classify the different types of rims according to their composition, we specified a minimum overall accuracy of 85% for the reconnaissance of the components

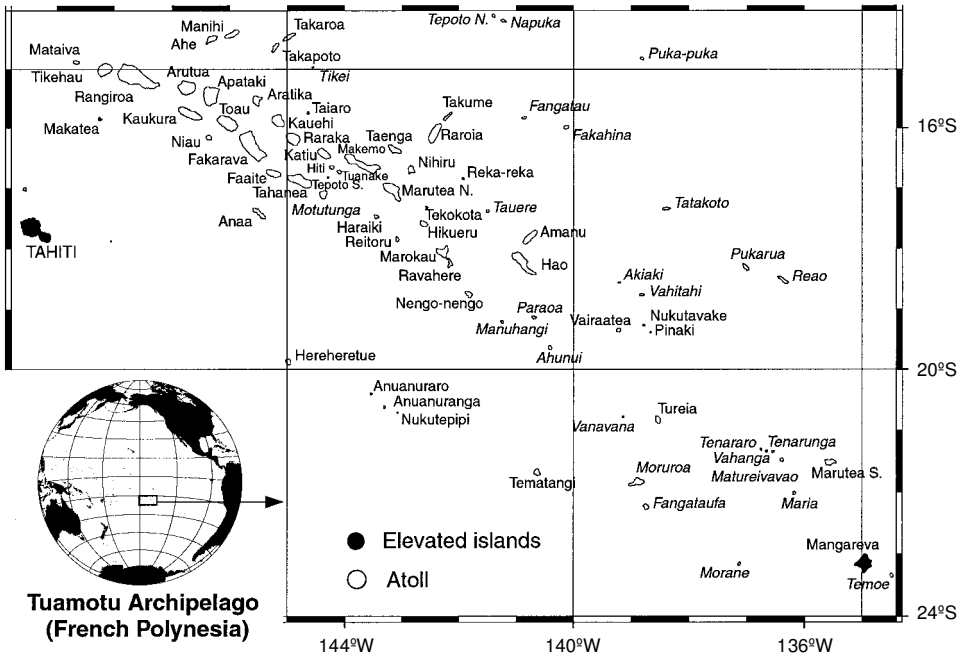

Figure 1. Location and map of the Tuamotu archipelago. Names in italic are atolls not completely covered by SPOT HRV imagery.

of the rims using SPOT HRV imagery. Despite the individual history of each atoll, their rims are made with the same set of geomorphological units that can be hierarchically clustered into broader classes relevant for a characterization at landscape scale. We propose in table 1 a three-level hierarchy. The first level—Landscape level—has only four classes: 'Vegetation', 'Intertidal', 'Submerged' and 'Emerged'. The second level—Integrated level—is made of 13 classes sketched in figure 2. These classes might be discriminated manually on SPOT HRV images by a photo-interpreter (figure 2), according to empirical rules based on colour, shape and relative location of the classes (Lequeux *et al.* 1995). The last level—Unit level—is made of the geomorphological units traditionally described in coastal geomorphology literature (Battistini *et al.* 1975, Guilcher 1988). The size of these units can be quite small (few square metres). The 85% accuracy threshold is likely unreachable using SPOT-HRV images (20 m resolution) at the Unit level, but this level is useful for describing the composition of the Landscape and Integrated levels using conventional terminology.

To test how precisely the classes at Landscape or Integrated levels can be recognized in the three-dimensional spectral space (XS1, XS2, XS3), we used two supervised algorithms: (1) a simple algorithm based on a normalized Euclidian distance d_N (Poujade 1994) (2) an algorithm based on an adaptive Mahalanobis distance d_M (Celeux *et al.* 1989). The Poujade algorithm requires the mean and variance of each class in each spectral band. The distance $d_N(p, (\mu, \sigma))$ between a pixel p and the class represented by its mean and variance (μ, σ) is computed using:

$$d_N^2(p, (\mu, \sigma)) = \sum_{k = XS1 \ldots XS3} \frac{(p_k - \mu_k)^2}{\sigma_k} \qquad (1)$$

The adaptive algorithm requires the 3×3 covariance matrix for each class. The

Table 1. Three levels of description for an atoll rim. The size of the objects at the Landscape and Integrated levels is compatible with the spatial resolution of SPOT-HRV multispectral images (20 m). Most of the Units are defined in Battistini *et al.* (1975). 'Kopara pond' are cyanobacterian ponds, located in stagnation zones.

Landscape level 4 categories	Integrated Level 13 categories	Unit level
Vegetation	Vegetation	Vegetation (bush, trees)
Emerged domain (without vegetation)	Conglomerate	Conglomerate
	Coral rubble	Boulder rempart
		Detrital ridge
		Shingle spread
		Shingle spread over conglomerate
	Soils	Soils
Intertidal domain	Intertidal reef flat	Soils with old shingle spread
		Intertidal reef flat
		Intertidal inner reef flat
		Algal ridge
	Intertidal coral rubble	Beach
		Spillway spit
		Hydraulic bank
		Littoral spit
	Intertidal conglomerate	Intertidal conglomerate
		Fossil algal ridge
		Old reef spit (feo)
		Eroded conglomerate
	Residual spillway	Residual kopara pond
		Cyanobacterian mats
		Residual spillway flagstone
Submerged domain	Deep water >1 m depth	Lagoon
		Inner slope
		Outer slope
		Pass
	Spillway	Functional spillway
		Submerged rim
	Submerged reef flat	Submerged outer reef flat
		Submerged inner reef flat
	Enclosed lagoon	Enclosed lagoon
	Kopara pond	Kopara pond

distance $d_M(p, (\mu, \sigma))$ between a pixel p and the class represented by its mean and covariance matrix (μ, C) is computed using:

$$d^2_M(p, (\mu, C)) = |C|^{1/3}(\mu - p)^t C^{-1}(\mu - p) \quad (2)$$

where $|C|$ is the determinant of the matrix C.

The test was performed using a SPOT HRV image of Tikehau atoll (figure 3) acquired in July 1994. Tikehau is morphologically very diversified (Intes *et al* 1995). All the classes at Unit level are encountered along its rim. Therefore, Tikehau may be considered as a good test atoll. Training and control areas were identified and georeferenced for all the classes at Integrated and Landscape levels (figure 3), during field trips carried out in June 1994, July 1994 and December 1995. The number of

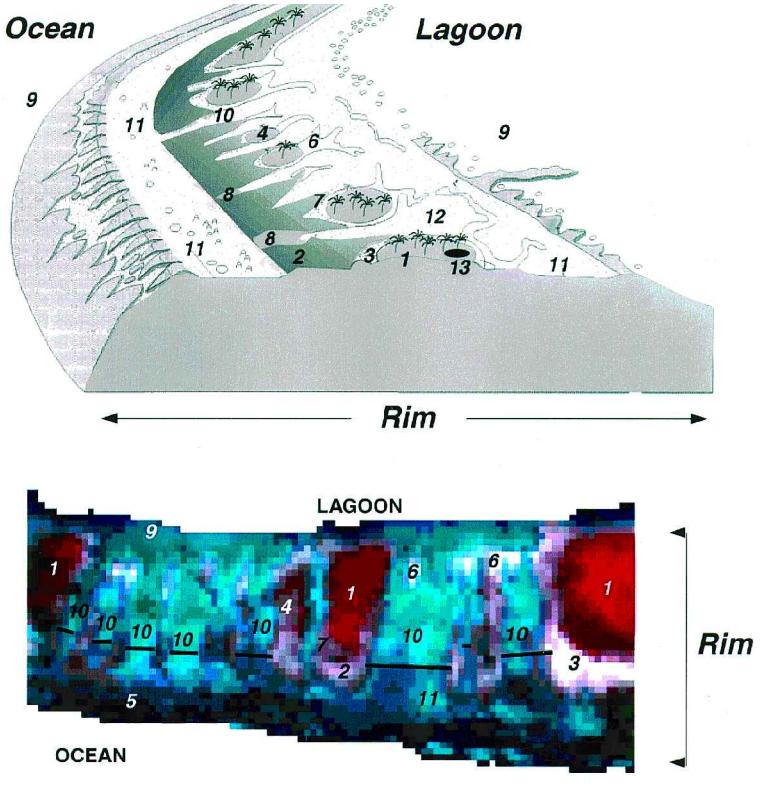

Figure 2. Bloc-diagram of an atoll rim (from Battistini *et al.* 1975) displaying the 13 classes at the Integrated level of description. The classes are also readily visible on a SPOT HRV image of the rim of the Tikehau atoll. The black segments indicate the locations of the apertures in this rim with numerous spillways. The aperture A is simply the sum of the width of these segments.

training pixels used to determine the statistical properties of the classes range between 44 (for kopara) to 500 (deep water). Generally, individual training or control stations were clusters made of 5 to 20 pixels. The accuracy of the two algorithms was quantified by the overall accuracy of the normalized confusion matrices (Zhuang *et al.* 1995). The 95% confidence interval of the overall accuracy is computed assuming a normal distribution (Ma and Redmond 1995).

After the calibration stage based on Tikehau atoll, a set of 117 segments of rims with various lengths and widths but with uniform exposure was processed at the Landscape level. The segments belong to 14 atolls differing in size, shape, latitude and longitude and of course morphology (figure 4 and table 2). The selection of the atolls is explained in detail in Dufour and Harmelin-Vivien (1997). They were surveyed during the Typatoll 1 cruise in November 1994. The processing of each segment provides a surface of 'Intertidal', 'Submerged', 'Emerged' and 'Vegetated' classes, with an overall accuracy greater than 85%. The surfaces covered by the different classes were normalized by the surface of the segment (table 3). Using these normalized surfaces, the segments

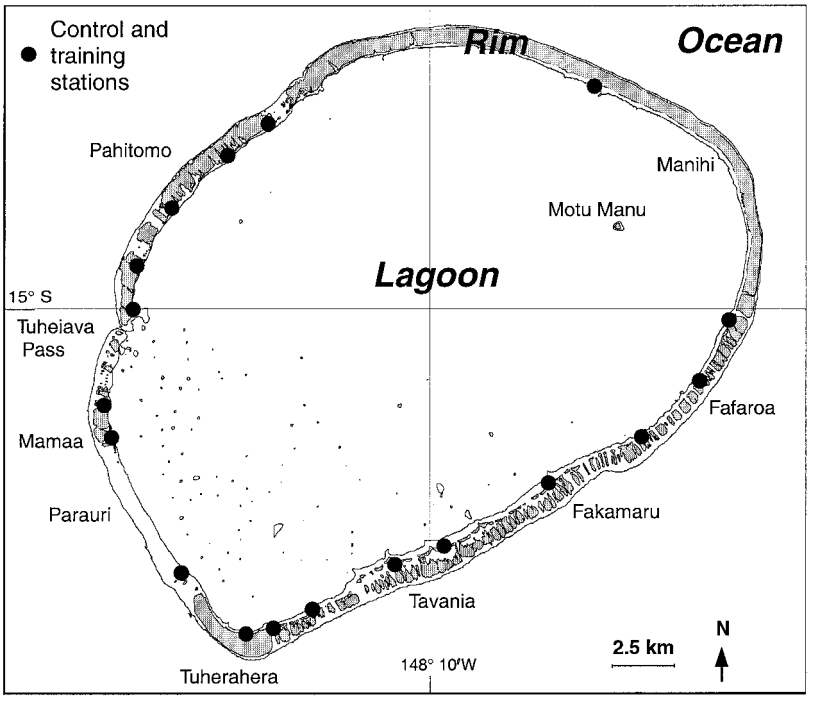

Figure 3. Map of Tikehau atoll with locations of the training and control areas. The domains 'Emerged' and 'Vegetation' are grey. 'Intertidal' and Submerged' domains are white.

were clustered using a hierarchical algorithm based upon Ward's method—i.e. criteria of minimum variance clustering—(Ward 1963) to define a typology of rims.

2.2. *Degree of aperture and exposure of the type of rims*

An indication of the aperture of the atoll is given by a one-dimensional variable: aperture A (in metres). At the Unit level, A is the sum of the width of the different spillways, submerged rims and passes (figure 2). At the Landscape level, aperture A is defined by the width of 'Submerged' area of the rim connecting the ocean and the lagoon. We define a simple index of degree of aperture ($A\%$) i.e. the ratio of A to the perimeter of the atoll p.

$$A\% = A/p \tag{3}$$

We also define the aperture $A_r\%$ of a given segment of rim r as:

$$A_r\% = \mathrm{A}_r/p_r \tag{4}$$

To test the null-hypothesis of equality of aperture between clusters of rims, an analysis of variance (ANOVA) was performed (Scherrer 1984). If the null-hypothesis must be rejected, an *a posteriori* Scheffe test determines which clusters differ in $A_r\%$. To obey the conditions of the ANOVA, $A_r\%$ was transformed to Arcsin($\sqrt{A_r\%}$) to insure homoscedasticity (i.e. homogeneity of the variances between clusters of rims) and an F-test was applied to insure normal distribution of this new variable (Zar 1984).

Exposure of a segment of rim is simply defined by the angle between the northern direction and the perpendicular to the oceanic side of the rim. To test whether the different clusters of rims are linked to one exposure, a circular statistical analysis

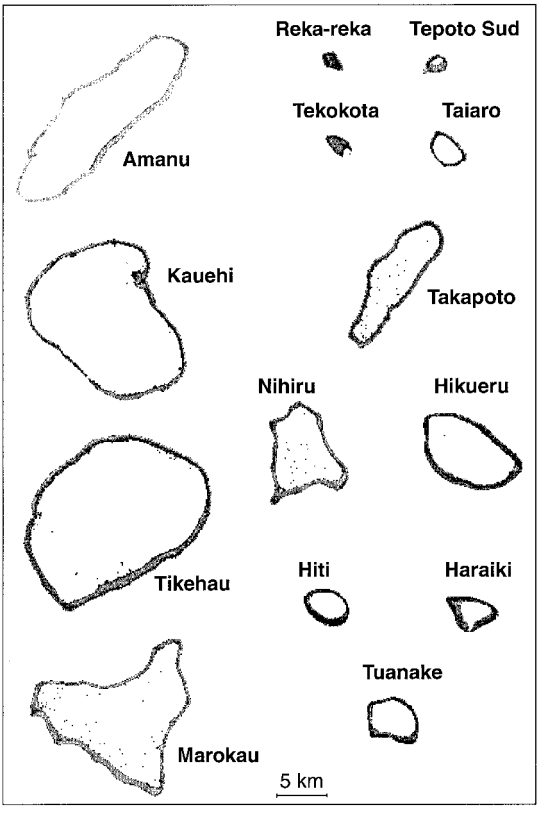

Figure 4. Diversity in size, shape and orieintation of the 14 selected atolls used to classify the type of rims. Scale is uniform.

Table 2. General features of the 14 atolls used to cluster the rims. The 'index of shape' is the 'Miller's circularity ratio', equal to Surface/(2πPerimeter^2) (Stoddart 1965). This index tends towards 1 for circular atolls and to 0 for complex-shaped or elongated atolls. The variable 'number of segments' is the number of segments with uniform exposure used to cluster the rims. A circular atoll is segmented into eight segments.

Atolls	Total surf. (km^2)	Aperture (A%)	Perimeter (km)	Latitude (°S)	Longitude (°W)	Rim surf. (km^2)	Number of segments	Index of shape
Amanu	244.0	0.29	72.5	17.8093	140.7671	34	10	0.584
Haraiki	25.4	0.23	19.8	17.4696	143.4476	15	5	0.816
Hikueru	107.0	0.25	40.0	17.5860	142.6127	24.6	10	0.840
Hiti	25.5	0.26	18.4	16.7309	144.0898	10.3	8	0.949
Kauehi	343.4	0.24	71.1	16.0409	145.0066	28.3	10	0.853
Marokau	256.0	0.22	75.0	18.0555	142.2844	38.5	14	0.572
Nihiru	100.2	0.34	45.2	16.7014	142.8362	20.7	13	0.616
Reka-reka	5.2	0.02	8.7	16.8401	141.9252	4.4	4	0.858
Taiaro	17.2	0.00	15.6	15.7445	144.6333	5.4	7	0.898
Takapoto	104.1	0.03	47.8	14.6313	145.2102	23	7	0.572
Tekokota	7.3	0.56	10.3	17.3153	142.5646	2.2	7	0.864
Tepoto	6.1	0.21	9.0	16.8166	144.2833	4.5	8	0.954
Tikehau	448.8	0.25	79.1	15.0141	148.1694	54.5	8	0.900
Tuanake	38.0	0.31	23.8	16.6434	144.2187	12.3	6	0.845

Table 3. Morphological variables available for each segment of rim.

Variable	Definition
Surfrim	Surface
V_r	Surface of vegetation class
I_r	Surface of intertidal class
E_r	Surface of emerged class
S_r	Surface of submerged class
$V_r\% = V_r/Surfrim$	Percentage of vegetation class
$I_r\% = I_r/Surfrim$	Percentage of intertidal class
$E_r\% = E_r/Surfrim$	Percentage of emerged class
$S_r\% = S_r/Surfrim$	Percentage of submerged class
P_r	Length along the reef crest
A_r	Aperture
$A_r\% = A_r/P_r$	Degree of aperture

was performed (Zar 1984). The null-hypothesis of no-directionality was tested for each type of rim with the non-parametric Rayleigh test and the distribution z_{α^n} (table B32 in Zar 1984). The Rayleigh test is based on the calculus of z:

$$X = \frac{\sum_{i=1}^{n} \cos a_i}{n};\ Y = \frac{\sum_{i=1}^{n} \sin a_i}{n};\ r_v = \sqrt{X^2 + Y^2};\ z = n.r_v^2 \tag{5}$$

where n is the number of segments, a_i is the exposure of the segment i, r_v is the length of the mean vector v. If the null-hypothesis is rejected ($z > z_{\alpha^n}$), the unimodal exposure is the angle a_v of the mean vector v with:

$$\cos a_v = \frac{X}{r_v};\ \sin a_v = \frac{Y}{r_v} \tag{6}$$

3. Results

3.1. *Image clustering*

At the Landscape level, the overall accuracy were $88.4\% \pm 1.62$ (95% confidence interval) for the Poujade algorithm and $90.32\% \pm 1.49$ for the adaptive algorithm. The difference in accuracy was not significant. For the Integrated level, none of the algorithms reached the required threshold of 85% accuracy. The Poujade and adaptive distance algorithms obtained $74.1\% \pm 2.2$ and $83.5\% \pm 1.9$ respectively. The different parametric representations of the 13 classes of the Integrated level are sketched in figure 5 for the two selected algorithms. This figure illustrates how the classes are spread in the spectral space defined by XS1, XS2, XS3. We show only the plan defined by the axis XS1, XS3 because the spectral features of the classes in XS1 and XS2 were very correlated. The ellipsoids at the top of figure 5 visualize the spectral space included in a distance d_N equal to 1.5σ, where σ is the variance of the considered class. The choice of the factor 1.5 is arbitrary, but for visualization purposes, it provides a good compromise between excessively small ellipsoids and those with too much overlap between them. The bottom of figure 5 presents limits defined by $d_M = 1.5\sigma$, with ellipsoids oriented in the direction given by the eigen vectors of the matrix C^{-1}. This figure helps explain the difference in accuracy between the two algorithms. The adaptive algorithm is based on more realistic assumptions that are well highlighted by the allure of the ellipsoids.

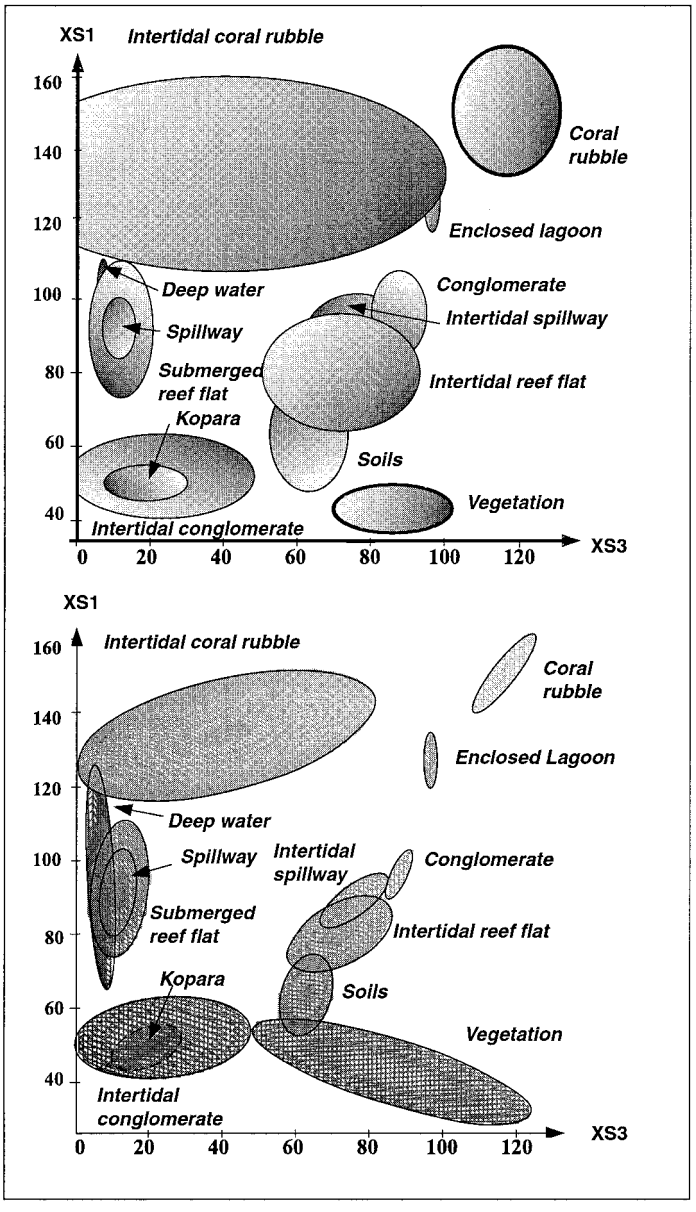

Figure 5. Parametric representation (see Results section for explanation) of the 13 categories at the 'Integrated' level of description of atoll rims. Top: Poujade algorithm. Bottom: adaptive algorithm.

The 83.5% accuracy for the adaptive algorithm was close to the specified level, but this rate was not consistently obtained. Indeed, if we decreased the number of training pixels randomly in the different classes, the accuracy actually ranged between 83.5% and 70.2%. For the pilot-atoll of Tikehau, a detailed ground truth was available and the sizes of training areas were consistent with the minimal specifications given by Hay (1979) to assess the accuracy of a classification. In other atolls, training will likely not be as extensive as in Tikehau because of logistic constraints.

Therefore, we had to conclude that the Tikehau's 83.5% accuracy is not easily reproducible. The 85% accuracy was unrealistic at the Integrated level and we could only consider the Landscape level. Since the Poujade algorithm is less time-consuming and requires less information than the adaptive algorithm, we used it to quantify the structures of rims using the Landscape level at an overall 85% accuracy. The normalized confusion matrix obtained at the Tikehau atoll using the Poujade algorithm at Landscape level is presented in table 4.

3.2. *Typology of rims*

We processed the 117 segments of rims using the Poujade algorithm. We obtained for each segment of rim r the variables $V_r\%$, $I_r\%$, $E_r\%$ and $S_r\%$ defined in table 3. The dendrogramm (not presented here, because it included 117 elements) of the hierarchical clustering of these four variables provided nine final clusters, simply called Rim1 ... Rim9. The histograms in figure 6 emphasize the difference in structure according to $V_r\%$, $I_r\%$, $E_r\%$ and $S_r\%$. Figure 7 visualizes what these rims look like, using for each type of rim a sample extracted from one of the 14 studied atolls.

3.3. *Type of rims and aperture*

Figure 7 visualizes an *a priori* gradient of aperture between rims, from a maximum (Rim4) to a minimum (Rim1). The results of ANOVA for the variable Arc $\sin(\sqrt{A_r\%})$ were highly significant (degree of freedom = 8–108; F-value = 40.008; $p = 0.001$) and the null-hypothesis of equality of the aperture was rejected. The *a posteriori* Scheffe test ($p = 0.05$) highlighted three groups of rims that synthesize the gradient of aperture:

- Aper1: including Rim1, Rim8, Rim9;. $A_r\% = 0.02 \pm 0.04$ (average $\pm$ standard deviation, negative values have no signification, minimum is 0) ($n = 59$).
- Aper2: including Rim2, Rim3, Rim5, Rim6, Rim7; $A_r\% = 0.40 \pm 0.19$ ($n = 43$).
- Aper3: including Rim4; $A_r\% = 0.67 \pm 0.22$ ($n = 15$).

3.4. *Type of rim and exposure*

The circular scatter diagrams in figure 8 indicate the exposure of the samples for each type of rim. The direction of the mean vector demonstrates the preferential exposure. The length of the mean vector varies inversely with the amount of dispersion. Table 5 shows the results of circular statistical analysis for the nine groups of rims. Eight groups have significantly a unimodal exposure ($p = 0.05$).

Table 4. Normalized confusion matrix for the Landscape level, using the Poujade algorithm. Overall accuracy is 0.88.

	Reference			
	Submerged	Intertidal	Emerged	Vegetation
Submerged	0.851	0.111	0.022	0.016
Intertidal	0.185	0.805	0.005	0.004
Emerged	0.000	0.071	0.928	0.001
Vegetation	0.001	0.042	0.005	0.952

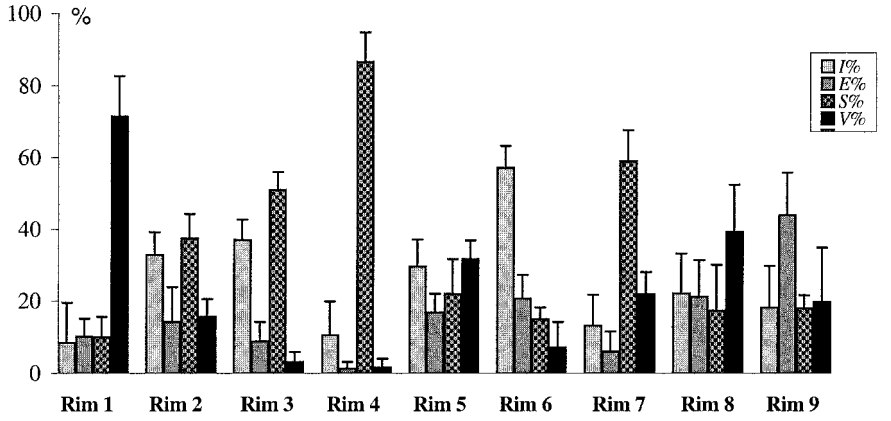

Figure 6. For each type of rim: mean+standard deviation (in percentage) of the vegetation ($V\%$), intertidal ($I\%$), emerged ($E\%$) and submerged ($S\%$) classes.

4. Discussion

Our rim typology is based on the four variables at the Landscape level. The performance of more complex algorithms for the recognition of classes at the 'Integrated' level or even for classes at the 'Unit' level was assessed. It is possible to reach the 85% accuracy, but with much more complex analysis that require fuzzy classification and knowledge-based algorithms characterizing the spatial relationships between classes. An example of such a complex study is described in Andréfouët and Roux (1998), for the reconnaissance of kopara ponds surrounded by vegetation. In this study, our objectives were not to provide detailed maps of the rims or inventories of specific units, but to retrieve landscape parameters (degree of aperture) useful for linking external oceanic forcing with lagoon functioning. We were more interested in a summary of the relevant structural properties of the rims rather than detailed information. The precision of the description of a rim at the Landscape level was adequate for our purpose despite its simplicity. Complementary tests not described here show that aperture quantified at the Integrated or Landscape level are very close. Moreover, other tests on Tikehau showed that aperture computed from aerial photos and SPOT HRV images does not differ more than 8%. Therefore, a higher resolution will likely not modify our typology from the point of view of aperture, a conclusion that may not be applied to other ecosystems and problems (Benson and MacKenzie 1995). However, for future studies such as inventories of specific units (kopara or underwater habitats for fisheries), the Landscape level most likely will be too imprecise and irrelevant.

The hydrological characteristics of oceanic water bathing the Tuamotu archipelago are rather stable throughout the year, being located in the South Pacific Gyre (Rancher and Rougerie 1995). Easterly tradewinds are dominant with a decrease during the rainy season. Dominant swell year round comes from a general southerly direction but the most energetic swells come from south-west. Northern swells coming from North Pacific occur frequently between November and March, but with lower amplitude. Tidal amplitude is very low all along the archipelago with a range between 0.3 m and 0.5 m. Table 6 shows that most of the types of rim identified using the Landscape level have a preferential exposure. Therefore, structure of rims and exposure are statistically linked, suggesting direct causal relationships according to the direction of dominant swell. Rims 3, 4, 6 and 7 are exposed to the southern swell.

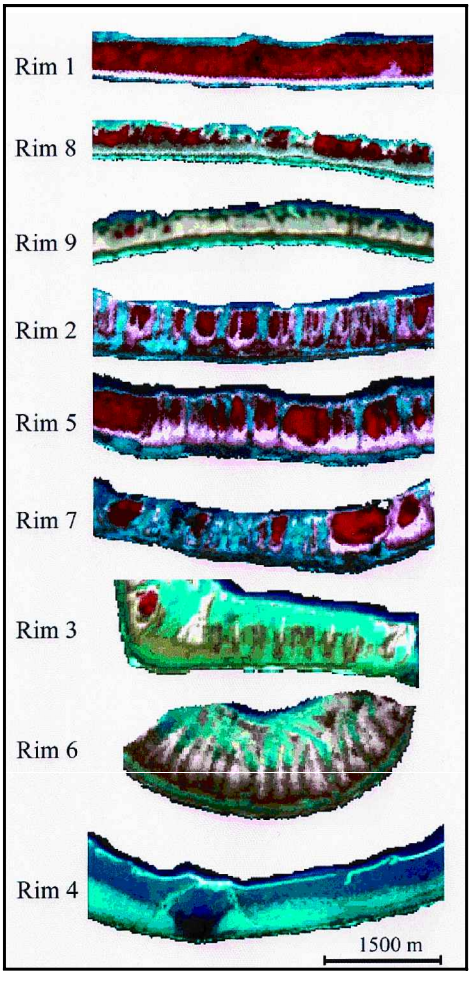

Figure 7. Samples of the nine types of rims viewed by SPOT-HRV images. The segments of rim have been rotated to display lagoon-side on top. From top to bottom, according to a gradient of aperture: Rims 1, 8, 9, 2, 5, 7, 3, 6 and 4. Vegetation ($V\%$) appears red; intertidal ($I\%$) is brown to black, emerged ($E\%$) is white to grey; and submerged ($S\%$) is blue-green.

Their coarse structure (dominant submerged or intertidal areas, figure 5) is the result of the permanent erosion from swell action over long time-scale period. Erosion processes on atoll rims are evidenced by broken up conglomerate along the outer reef flats or spillways (Montaggioni and Pirrazoli 1984). These signs are present for Rims 3, 6 and 7 while the conglomerate is still present in less open Rims 1, 8, 9 or 5 that are also mostly in the northern direction. On Rim 4, field studies show that the conglomerate does not exist anymore in large areas, except for rims lightly uplifted by tectonic processes such as Rangiroa atoll (Stoddard 1969). On the other hand, the most protected and vegetated rims (Rim 1 and 8) are exposed to the north. The unvegetated and closed Rim9 is exposed to the east, but we suggest it may be due to hurricanes rather than tradewinds. The semi-open rims (Rim 5, 2) are exposed to the south-east and to the north-west respectively, i.e. intermediate directions between north and south.

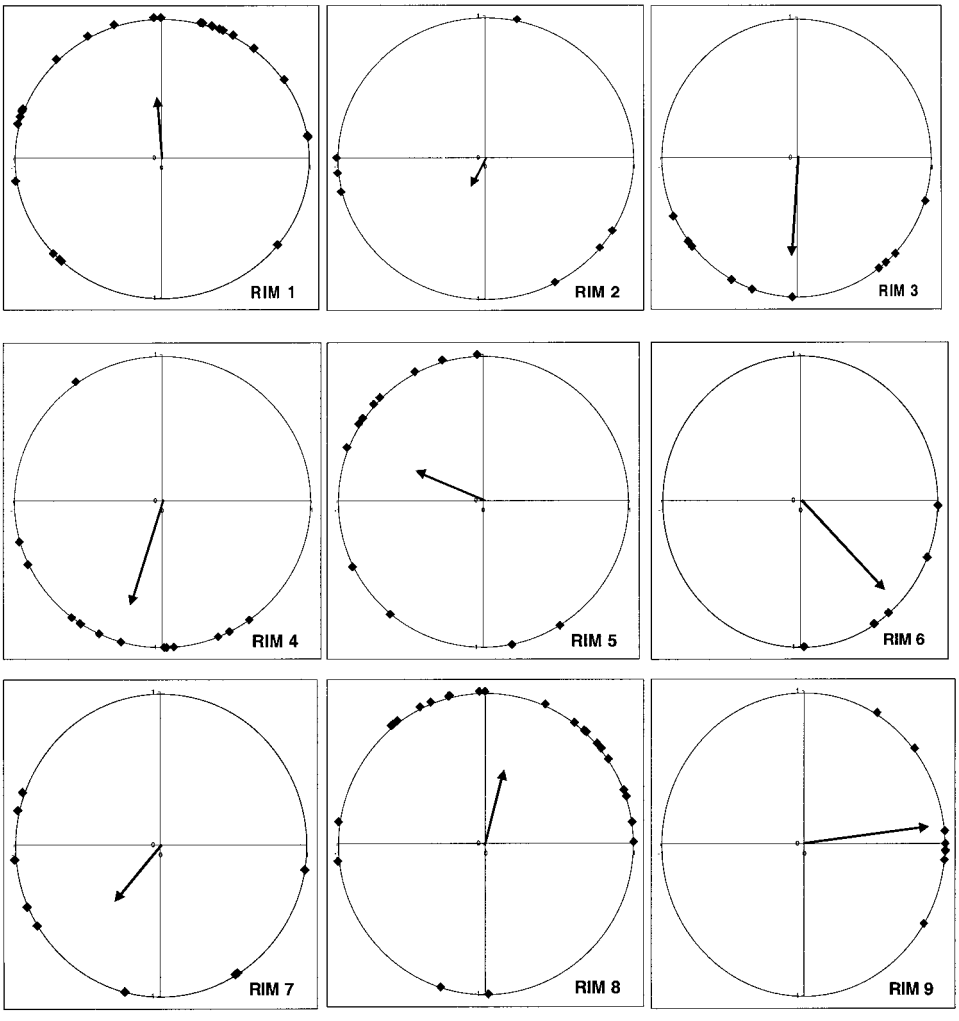

Figure 8. For each type of rim: circular scatter diagrams of the exposure of the samples. The direction of the arrow is the mean exposure. Its length is proportional to the dispersion of the samples.

Table 5. Results of the Rayleigh test for the circular analysis for each type of rim (s = significant, ns = non significant).

	Rim1	Rim2	Rim3	Rim4	Rim5	Rim6	Rim7	Rim8	Rim9
X	− 0.029	− 0.093	− 0.039	− 0.218	− 0.471	0.624	− 0.319	0.131	0.892
Y	0.448	− 0.201	− 0.702	− 0.723	0.217	− 0.607	− 0.369	0.501	0.104
n	27	7	10	15	12	5	9	24	8
z computed	5.451	0.344	4.948	8.576	3.238	3.794	2.150	6.444	7.264
z_{α^n} theoretic	2.968	2.885	2.919	2.945	2.932	2.863	2.910	2.964	2.910
Signification ($p = 0.05$)	s	ns	s	s	s	s	ns	s	s

Table 6. Percentage of each type of rim in 49 atolls of the Tuamotu archipelago and number of segments with uniform exposure. Among the 51 atolls covered by the SPOT HRV, two atolls (Makatea—uplifted and Nukutavake—dry lagoon) do not have a typical saucer-shape morphology and are not included.

Atoll	Lat. (°S)	Long. (°W)	Nb. Segments	Rim1	Rim2	Rim3	Rim4	Rim5	Rim6	Rim7	Rim8	Rim9
Ahe	14.4893	146.3211	7	0.06	—	—	—	0.69	—	—	0.25	—
Amanu	17.8093	140.7671	10	0.09	0.31	0.20	—	0.27	0.13	—	—	—
Anaa	17.4053	145.4902	7	0.09	—	—	—	0.39	—	0.52	—	—
Anuanuranga	20.6210	143.3040	8	—	—	0.36	—	0.36	—	—	0.11	0.17
Anuanuraro	20.4037	143.5359	4	—	—	0.29	—	—	—	0.25	0.25	0.21
Apataki	15.4518	146.3153	7	—	—	0.22	—	0.09	—	0.24	0.25	0.20
Aratika	15.5339	145.5143	8	0.26	—	0.34	—	0.11	—	0.29	—	—
Arutua	15.3147	146.7370	10	—	—	—	0.36	0.05	—	0.47	—	0.12
Faaite	16.7531	145.2383	8	—	—	0.23	0.32	0.45	—	—	—	—
Fakarava	16.2954	145.5951	10	0.26	—	0.12	0.39	0.10	—	0.13	—	—
Hao	18.2449	140.8729	14	0.26	0.32	0.14	—	0.11	—	0.05	0.09	0.03
Haraiki	17.4696	143.4476	5	0.41	—	0.32	—	—	—	0.27	—	—
Hereheretue	19.8765	144.9820	6	0.11	—	0.28	0.19	—	—	0.27	—	0.15
Hikueru	17.5860	142.6127	10	—	0.14	—	0.42	0.11	—	—	0.33	—
Hiti	16.7309	144.0898	8	0.23	0.06	0.08	0.35	0.28	—	—	—	—
Katiu	16.4280	144.3558	7	—	—	0.48	—	0.28	—	—	0.24	—
Kauehi	16.0409	145.0066	10	0.56	—	—	0.11	0.22	—	0.11	—	—
Kaukura	15.7529	146.6742	8	—	—	—	0.39	—	—	0.61	—	—
Makemo	16.4515	143.1598	13	0.24	—	0.12	0.39	0.12	—	—	0.13	—
Manihi	14.4032	145.9622	7	—	—	—	—	0.48	—	0.06	0.08	0.38
Marokau	18.0555	142.2844	14	0.20	0.11	—	0.22	0.32	—	0.15	—	—
Marutea Nord	17.0410	143.1585	11	—	—	—	0.53	0.26	—	0.11	—	0.10
Marutea Sud	21.5179	135.5601	11	0.06	0.07	—	—	0.23	—	0.64	—	—
Mataiva	14.8827	148.6702	5	0.60	—	—	—	0.40	—	—	—	—
Nengo-nengo	18.7601	141.8310	7	—	—	0.36	0.14	0.21	—	—	0.08	0.21
Niau	16.1546	146.3605	6	1.00	—	—	—	—	—	—	—	—
Nihiru	16.7014	142.8362	13	—	0.10	0.09	0.27	0.21	—	—	—	0.33
Nukutepipi	20.7120	143.0697	4	—	—	0.44	—	0.19	—	—	—	0.37
Pinaki	19.3880	138.6675	6	0.74	—	—	—	0.13	—	—	0.13	—
Rangiroa	15.1425	147.6058	18	0.07	0.02	0.12	0.05	0.28	—	0.41	0.05	—
Raraka	16.1843	144.8942	8	—	0.15	0.17	—	0.37	—	0.15	0.16	—
Raroia	16.0795	142.4289	9	—	0.36	—	0.07	0.48	—	—	0.05	0.04
Ravahere	18.2338	142.1695	9	—	—	0.39	0.05	0.20	—	—	0.36	—
Reitoru	17.8411	143.0832	6	—	—	0.11	0.18	0.36	—	—	0.19	0.16
Reka-reka	16.8401	141.9252	4	0.20	—	—	—	0.29	—	—	0.51	—
Taenga	16.3551	143.1331	5	—	0.10	0.21	—	—	—	0.24	—	0.45
Tahanea	16.8696	144.7749	12	—	—	0.08	0.36	0.29	—	0.27	—	—
Taiaro	15.7445	144.6333	7	0.33	—	—	—	0.00	—	—	0.67	—
Takapoto	14.6313	145.2102	7	0.55	—	—	—	0.26	—	—	0.19	—
Takaroa	14.4491	144.9697	10	0.26	—	—	—	0.33	—	0.13	0.28	—
Takume	15.7975	142.1966	6	—	—	0.08	—	0.19	—	0.73	—	—
Tekokota	17.3153	142.5646	7	0.19	—	0.30	0.25	—	—	0.11	0.15	—
Tematangi	21.6789	140.6356	7	—	0.16	—	—	0.23	—	0.22	0.28	0.11
Tepoto	16.8166	144.833	8	0.14	—	—	—	0.07	0.43	—	0.36	—
Tikehau	15.0141	148.694	8	0.22	0.33	—	—	0.21	—	0.24	—	—
Toau	15.9089	146.0405	8	—	—	—	0.40	0.14	—	0.46	—	—
Tuanake	16.6434	144.2187	6	—	0.19	0.30	—	0.19	—	—	0.14	0.18
Tureia	20.8263	138.5404	5	0.56	—	—	—	0.18	—	—	—	0.26
Vairaatea	19.3573	139.2273	4	0.40	0.29	—	—	—	—	0.31	—	—

Exposure to swells definitively explains both structure of the rims and degree of aperture. However, size and shape of the atolls are also co-factors. Indeed, complementary analysis not detailed here shows that the small ($<20\,km^2$) circular atolls may have a dominance of Rim 1 or Rim 8 rims on their southern part while it is unusual on larger atolls. In this study, the samples from Rim 1 and Rim 8 along the south belong to small atolls (i.e. Reka-Reka or Taiaro). The link between structure of the rims, exposure and patterns of swells prevent the generalization of our results to atolls located in other oceanic regions. While the typology of rims likely could be extended to the neighboring atolls of the Society Archipelago or Cook Islands, caution is required for atolls elsewhere in the Pacific Ocean (Melanesia, Micronesia, Australia and Hawaii) and of course atolls in the Indian Ocean and Caribbean. We suggest that similar work could be conducted in other homogeneous oceanic regions to have a complete characterization of the atolls worldwide.

The rim is the result of multi-secular processes of erosion and diagenesis. But, the rim also controls the fluxes of water between the ocean and lagoon at an /hour/day/week/month/year temporal scale, in conjunction with the variability in tide, wind, swell and season. The knowledge of the rim structure is a first step in estimating the fluxes at lagoon boundaries for inferring a residence time for the water inside different lagoons (Tartinville *et al.* 1997). Generally, in Tuamotu, flux of water through the rim overpowers other hydrodynamic processes of water exchange, except for completely closed atolls such as Taiaro. In this case, residence time results from equilibrium between precipitation, evaporation and groundwater flow inside the rim (Leclerc *et al.* 1999). Residence time is an important factor of control on the biological processes inside lagoons (Hamner and Wolanski 1988, Hatcher *et al.* 1997). Residence time of lagoonal water was correlated with phytoplanktonic biomass (Delesalle and Sournia 1992) and nutrient concentrations (Hatcher and Fritch 1985). In Tuamotu atolls, Dufour *et al.* (1998) reported a relationship between nutrient concentrations and degree of aperture, and therefore water residence time. The combination of both rim typology and *in situ* current measurements based on different swell conditions will lead to a better quantification of the mechanism of water renewal and on the biological functioning of atoll lagoons. Preliminary results are described in Andréfouët (1998). It shows the link between lagoonal chlorophyll concentrations and residence time computed using oceanic wave height derived from altimetry and measured water velocities in spillways located in different types of rims.

The typology of rims also provides wide-scale information to help people in charge of resource management for an entire atoll. Aquaculture of oysters for the production of black pearls, fisheries, coconut harvesting and tourism are the main sources of income for the few thousands of inhabitants of the Tuamotu archipelago. Tuamotu atolls are the subject of planning and management activities that have dramatically increased in the past fifteen years (Chenon *et al.* 1990). However, the managers lack synoptically consistent data to make their decisions. Three examples illustrate how the structure of an atoll rim can be helpful in selecting the locations of activities and prioritizing them:

- The government of French Polynesia is leading an inventory of the kopara ponds to assess the activities of their microbial communities for bio-technologies (Mao Che *et al.* 1998). Kopara ponds are encountered in different locations around rims, but the most interesting ones are found in stable environments that prevent the mixing of the different pond layers. These environments are only in Rim1, Rim8 and on the large vegetated islets of Rim7.

- Rim1 and Rim8 are more suitable for agricultural purposes. They allow construction of roads, while exploitation of Rim5 or Rim7 requires means of navigation. Large and stable rims likely have freshwater lens. The cost of exploitations will be higher in Rim2, Rim3, Rim4 and Rim6.
- The best 'atollscapes' for tourism are certainly located in Rim5 and Rim2 because of the succession of small islets and shallow submerged zones.

As a baseline for future classification of atolls for research or management, table 6 provides the proportion of each type of rim in the 49 atolls of the Tuamotu covered by the SPOT HRV imagery.

Acknowledgments

We thank the two reviewers for their constructive suggestions. This research was financially supported by Département de la Recherche et des Etudes Doctorales of the Centre Universitaire de Polynésie Française and by Programme National sur les Récifs Coralliens. We are grateful to Lionel Laurore for free access to the image processing software GEOIMAGE. We thank both IFREMER and the Territory of French Polynesia that provided the archive of SPOT images. The crew of the vessel Antarctica and members of the EMIR program are acknowledged for providing assistance in the field at Tikehau in July 1994. Thanks also to the crew of the French Navy vessel La Railleuse which hosted the Typatoll 1 cruise. Special thoughts for the inhabitants of Tikehau, especially Theodore Teakura and his family, for the help and hospitality given in June 1994 and December 1995.

References

Andréfouët, S., 1998, *Mécanismes de renouvellement des eaux des lagons d'atolls—Action de recherche 12 PGRN*. Report PGRN (Papeete: Service Ressources Marines).

Andréfouët, S., and Roux, L., 1998, Characterisation of ecotones using membership degrees computed with a fuzzy classifier. *International Journal of Remote Sensing*, **19**, 3205–3211.

Battistini, R., Bourrouilh, F., Chevalier, J.-P., Coudray, J., Denizot, M., Faure, G., Fisher, J. C., Guilcher, A., Harmelin-Vivien, M., Jaubert, J., Laborel, J., Masse, J.-P., Maugé, L. A., Montaggioni, L., Peyrot-Clausade, M., Pichon, M., Plante, R., Plaziat, J. C., Plessis, Y., Richard, G., Salvat, B., Thomassin, B., Vasseur, P., and Weydert, P., 1975, Eléments de terminologie récifale indopacifique. *Thétys*, **7**, 1–111.

Benson, B. J., and Mackenzie, M. D., 1995, Effects on sensor spatial resolution on landscape structure parameters. *Landscape Ecology*, **10**, 113–120.

Bourrouilh-Lejan, F. G., Tallandier, J., and Salvat, B., 1985, Early diagenesis from 6000 years ago and the geomorphology of atoll rims in the Tuamotu. In *Proceedings of 5th International Coral Reef Congress, Tahiti*, pp. 235–240.

Bourrouilh-Lejan, F. G., and Tallandier, J., 1985, Sédimentation et fracturation de haute énergie en milieu récifal: tsunamis, ouragans et cyclones et leurs effets sur la sédimentologie et la géomorphologie d'un atoll: motu et hoa, à Rangiroa, Tuamotu, Pacifique SE. *Marine Geology*, **67**, 263–333.

Bryan, E. H., 1953, Check list of atolls. *Atoll Research Bulletin*, **19**, 1–38.

Buigues, D., Gachon, A., and Guille, G., 1992, Mururoa atoll (French Polynesia). 1. Structure and geological evolution. *Bulletin de la Société Géologique de France*, **163**, 645–657.

Celeux, G., Diday, E., Govaert, G., Lechevallier, Y., and Ralambondrainy, H., 1989, *Classification automatique des données, environnement statistique et informatique* (Paris: Dunod).

Chenon, F., Varet, H., Loubersac, L., Grand, S., and Hauti, A., 1990, SIGMA POE RAVA, système d'informations géographique du Service de la Mer et de l'Aquaculture. Un outil de gestion du domaine public maritime pour la perliculture. In *Proceedings of Pix'Iles 90: International Workshop on Remote Sensing and Insular Environments in the Pacific: integrated approaches, Nouméa-Tahiti* (Noumea: ORSTOM), pp. 561–570.

DELESALLE, B., and SOURNIA, A., 1992, Residence time of water and phytoplankton biomass in coral reef lagoons. *Continental Shelf Research*, **12**, 939–949.

DUFOUR, P., and HARMELIN-VIVIEN, M., 1997, A research program for a typology of atoll lagoons: strategy and first results. In *Proceedings of 8th International. Symposium on Coral Reef, Panama* (Balboa: Smithsonian Institute), pp. 843–848.

DUFOUR, P., ANDRÉFOUËT, S., CHARPY, L., BONNET, S., and GARCIA, N., 1998, Nutrients concentrations in lagoons are dependant on atoll morphology. In *Proceedings of International Society for Reef Studies European Meeting, Perpignan-France* (Perpignan: EPHE), Vol. Abstracts, p. 66.

FORMAN, R. T. T., and GODRON, M., 1986, *Landscape Ecology* (New-York: John Wiley & Sons).

FOURGASSIÉ, A., 1990, La spatiocarte marine, une solution pour la cartographie des atolls polynésiens. In *Proceedings of Pix'Iles 90: International Workshop on Remote Sensing and Insular Environments in the Pacific: integrated approaches, Nouméa-Tahiti* (Noumea: ORSTOM), pp. 329–341.

FUMAS, M. J., MITCHELL, A. W., GILMARTIN, M., and REVELANTE, N., 1990, Phytoplankton biomass and primary production in semi-enclosed reef lagoons of the central Great Barrier Reef, Australia. *Coral Reefs*, **9**, 1–10.

GUILCHER, A., 1988, *Coral Reef Geomorphology* (New York: John Wiley & Sons).

HAMNER, W. M., and WOLANSKI, E., 1988, Hydrodynamics forcing functions and biological processes on coral reefs: a status review. In *Proceedings of 6th International Coral Reef Symposium*, Vol. 1 (Townsville: 6th Int. Coral Reef Symp. Executive Committee), pp. 103–114.

HATCHER, B. G., 1997, Coral reef ecosystems: how much greater is the whole than the sum of the parts? *Coral Reefs*, **16**, S77–S91.

HATCHER, A. I., and FRITCH, C. A., 1985, The control of nitrate and ammonium concentrations in a coral reef lagoon. *Coral Reefs*, **4**, 101–110.

HATCHER, B. G., IMBERGER, J., and SMITH, S. V., 1987, Scaling analysis of coral reef systems: an approach to problems of scale. *Coral Reefs*, **5**, 171–181.

HAY, A. H., 1979, Sampling designs to test land-use map accuracy. *Photogrammetric Engineering and Remote Sensing*, **45**, 529–533.

INTES, A., CAILLART, B., CHARPY-ROUBAND, C.-J., CHARPY, L., HARMELIN-VIVIEN, M., GALZIN, R., and MORIZE, E., 1995, Tikehau: an atoll of the Tuamotu Archipelago. *Atoll Research Bulletin*, **415**.

ITO, G., MCNUTT, M., and GIBSON, R. L., 1995, Crustal structure of the Tuamotu Plateau, 15°S, and implications for its origin. *Journal of Geophysical Research*, **100**, 8097–8114.

LECLERC, A. M., BAPTISTE, P., TEXIER, D., and BROC, D., 1999, Density induced water circulation in atoll coral reefs: a numerical study. *Limnology Oceanography*, **44**, 1268–1281.

LEQUEUX, D., ANDRÉFOUËT, S., and MOREL, Y., 1995, *Protocole de réalisation de produits cartographiques en milieu d'atolls. Photo-interprétation assistée par ordinateur à partir d'images SPOT et de photographies aériennes.* Report SPT (Papeete, Tahiti: Service de l'urbanisme/ IFREMER).

LOUBERSAC, L., 1994, Information géographique dérivée des données de la télédétection spatiale de haute résolution sur les lagons des îles hautes et des atolls. Application aux environnements des îles de la Polynésie Française: états et perspectives. *Mémoires de l'Institut Océanographique,* **18**, 75–85.

LOUBERSAC, L., DAHL, A. L., COLLOTTE, P., LEMAIRE, O., D'OZOUVILLE, L., and GROTTE, A., 1988, Impact assessment of cyclone Sally on the almost atoll of Aitutaki (Cook Islands) by remote sensing. In *Proceedings of 6th International Coral Reef Symposium*, Vol. 2 (Townsville: 6th Int. Coral Reef Symp. Executive Committee), pp. 455–462.

LOUBERSAC, L., BURBAN, P. Y., LEMAIRE, O., VARET, H., and CHENON, F., 1991, Integrated study of Aitutaki's lagoon (Cook Islands) using SPOT satellite data and *in situ* measurements: bathymetric modelling. *Geocarto International*, **6**, 31–37.

MA Z., and REDMOND, R. L., 1995, Tau coefficients for accuracy assessment of classification of remote sensing data. *Photogrammetric Engineering & Remote Sensing*, **61**, 435–439.

MAO CHE, L., ANDRÉFOUËT, S., GUYAUNEAUD, R., CAUMETTE, P., LE CAMPION, T., TRICHET, J., and PAYRI, C., 1998, Photosynthetic microbial communities and pigment composition of microbial mats (kopara) encountered in atolls of French Polynesia. Preliminary results. In *Proceedings of European Meeting, International Society for Reef Studies, Perpignan-France* (Perpignan: EPHE), Vol. Abstracts p. 118.

McNutt, M., and Menard, H. W., 1978, Lithospheric flexure and uplifted atolls. *Journal of Geophysical Research*, **83**, 1206–1212.

Menard, H. W., 1982, Influence of rainfall upon the morphology and distribution of atolls. In *The Ocean Floor*, edited by R. A. Scruton and M. Talwani (New York: John Wiley & Sons), pp. 305–311.

Montaggioni, L. F., and Pirazzoli, P., 1984, The significance of exposed conglomerates from French Polynesia (Pacific Ocean) as indicators of recent sea-level changes. *Coral Reefs*, **3**, 29–42.

Montaggioni, L., Richard, G., Bourrouilh-Le Jan, F., Gabrie, C., Humbert, L., Monteforte, M., Nairn, O., Pavri, C., and Salvat, B., 1985, Geology and marine biology of Makatea, an uplifted atoll, Tuamotu archipelago, Central Pacific Ocean. *Journal of Coastal Research*, **1**, 165–171.

Mumby, P., Raines, P., Gray, D., and Gibson, J., 1995, Geographic Information Systems: a tool for integrated coastal zone management in Belize. *Coastal Management*, **23**, 111–121.

Perrin, C., 1990, Genesis of atoll morphology—Mururoa (French Polynesia). *Comptes Rendus de l'Académie des Sciences Series II*, **311**, 671–678.

Pirazzoli, P. A., 1984, Cartographie des hauts fonds par télédétection dans l'archipel des Gambier (Polynésie française). *L'espace Géographique*, **3**, 277–284.

Pirazzoli, P. A., Montaggioni, L. F., Vergnaud-Grazzini, C., and Saliège, J. F., 1987, Late Holocene sea levels and coral reef development in Vahitahi atoll, eastern Tuamotu islands, Pacific Ocean. *Marine Geology*, **76**, 105–116.

Pirazzoli, P. A., Koba, M., Montaggioni, L. F., and Person, A., 1988a, Anaa (Tuamotu islands, central Pacific): an incipient rising atoll? *Marine Geology*, **82**, 261–269.

Pirazzoli, P. A., Montaggioni, L. F., Salvat, B., and Faure, G., 1988b, Late Holocene sea-level indicators from twelve atolls in the central and eastern Tuamotu (Pacific Ocean). *Coral Reefs*, **7**, 57–68.

Poujade, V., 1994, Reconnaissance des formes en télédétection, application à la cartographie planimétrique. PhD dissertation Université Paris VII.

Quattrochi, D. A., and Pelletier, R. E., 1990, Remote sensing for analysis of landscapes: an introduction. In *Quantitative methods in landscape ecology: the analysis and interpretation of landscape heterogeneity*, edited by M. G. Turner and R. H. Gardner (New-York: Springer-Verlag), pp. 51–76.

Rancher, J., and Rougerie, F., 1995, L'environnement océanique de l'archipel des Tuamotu (Polynésie Française). *Oceanologica Acta*, **18**, 43–60.

Salvat, B., Salvat, F., and Loubersac, L., 1990, Imagerie satellitaire SPOT et caractérisation géomorphologique des atolls: d'une étude de cas (Nukutepipi, Tuamotu) à la généralisation. In *Proceedings of Pix'Iles 90: International Workshop on Remote Sensing and Insular Environments in the Pacific: integrated approaches, Nouméa-Tahiti* (Noumea: ORSTOM), pp. 573–576/705–711.

Scherrer, B., 1984, *Biostatistiques*(Chicoutimi: Gaetan-Morin).

Stoddart, D. R., 1965, The shape of atolls. *Marine Geology*, **3**, 369–383.

Stoddart, D. R., 1969, Reconnaissance geomorphology of Rangiroa atoll, Tuamotu archipelago. *Atoll Research Bulletin*, **125**, 2–44.

Stoddart, D. R., and Murphy, F. J., 1996, Relative sea level history on two adjacent atolls, Northwest Tuamotu archipelago. In *Proceedings of 8th International Symposium on Coral Reef, Panama* (Balboa: Smithsonian Institute), Vol. Abstract p. 189.

Tartinville, B., Deleersnijder, E., and Rancher, J., 1997, The water residence time in the Mururoa atoll lagoon: sensitivity analysis of a three-dimensional model. *Coral Reefs*, **16**, 193–203.

Ward, J. H., 1963, Hierarchical grouping to optimize an objective function. *Journal of American Statistics Association*, **58**, 236–244.

Winterer, E. L., 1998, Cretaceous karst guyots: new evidence for inheritance of atoll morphology from subaerial erosional terrain. *Geology*, **26**, 59–62.

Woodroffe, C., McLean, R., Smithers, S., and Lawson, E., 1999, Atoll reef-island formation and response to sea-level change: West island, Cocos (Keeling) Islands. *Marine Geology*, **160**, 85–104.

Zar, J. H., 1984, *Biostatistical Analysis* (Englewood Cliffs, New Jersey: Prentice Hall).

Zhuang, X., Engel, B. A., Xiong, X., and Johannsen, C. J., 1995, Analysis of classification results of remotely sensed data and evaluation of classification algorithms. *Photogrammetric Engineering and Remote Sensing*, **61**, 427–433.